Water affinity guided tunable superhydrophobicity and optimized wettability of selected natural minerals

H Alptekin et al.

Original citation & hyperlink:
Alptekin, Hande, et al. "Water affinity guided tunable superhydrophobicity and optimized wettability of selected natural minerals." *Journal of Coatings Technology and Research* 16.1 (2019): 199-211.
https://dx.doi.org/10.1007/s11998-018-0115-y

ISSN 1547-0091

Publisher: Springer

The final publication is available at Springer via https://dx.doi.org/10.1007/s11998-018-0115-y

Water affinity guided tunable superhydrophobicity and optimized wettability of selected natural minerals

Hande Alptekin[a], *Emre Arkan*[1b,], *Cebrail Özbek*[b], *Mustafa Can*[b, *], *Amir Farzaneh*[a, **], *Mücahit Sütçü*[a,***], *Salih Okur*[a] *and Andrew J. Cobley*[c]

[a] Deparment of Materials Science and Engineering, Faculty of Engineering and Architecture, İzmir Katip Çelebi University, İzmir, Turkey
[b] Deparment of Engineering Sciences, Faculty of Engineering and Architecture, İzmir Katip Çelebi University, İzmir, Turkey

[c] The Functional Materials Research Group, Centre for Manufacturing and Materials Engineering, Faculty of Engineering Environment and Computing, Coventry University, Priory Street, Coventry CV1 5FB, UK

[1] Emre Arkan tel: +902323293535/3757, arkanemre@gmail.com

Abstract

We present a feasible methodology to prepare nonwetting surfaces from natural minerals. Various ranges of silanes were used for the surface grafting and the best customization was achieved by monochlorosilane. Water affinity analysis of surface functionalized diatomaceous earth was the key aspect of loading tunable wettability on particle surface. Covalent attachment was confirmed via X-ray photoelectron spectroscopy (XPS), while thermogravimetric analysis, nitrogen adsorption isotherms, and contact angle measurements were used for the evaluation of grafting density and other fundamental features of hydrophobic particles. Diatomaceous earth was chosen as a prototype to develop an efficient strategy for surface modification which can be apposite to another natural particle, so-called talc, which represents dichotomic performance to water. The present study paves the way for a new approach that can be employed to any proper inherent texture for the production of superhydrophobic powders.

Keywords: Tunable Wettability, Superhydrophobic Minerals, Water Affinity, Surface Grafting, Diatomaceous Earth

1. Introduction

Strong research interest has been shown in the development of low-cost and highly efficient superhydrophobic (SH) natural particles to replace their refined counterparts due to their contributions to surface energy and their unparalleled ability to repel water [1-8]. Superhydrophobic materials generally have a low surface energy with a contact angle (CA) greater than 150^{o} at room temperature (about 25 ^{o}C) and bind very weakly with drops of water resulting in the formation of water beads.[8-10] With regards to previous research, water droplets that are deposited on the surface interact with both constituent materials of the surface and the air confined within the structure; therefore, the spreading of a liquid on a structured surface is generally expressed with a Young's equation using interfacial free energy functions of three boundaries that are in turn solid-water-vapor [11, 12]. The desired water repellency can be attributable to strict regulation of key parameters that can repel the water and liquids even with remarkably lower surface energy values as in the case of many alcohols and alkanes [7]. Techniques to attain appropriate superhydrophobicity comprises PTFE coated carbon nanotubes to form flat surface arrays, lithographic methods to form periodic arrays of pillars, self-aligned polymer nanospheres and fluorinated polymers or long hydrocarbon chains as surface grafting articles [7, 9]. Such organic modifiers not only display increased hydrophobicity through driving low surface energy but also they can be impregnated to the surface of inherent structure such as natural minerals and textiles [7, 9, 13-17]. However, there have been no controlled studies which can be feasible as well as cost-effective to produce durable nonwetting surfaces from unprocessed and "as-received'' natural minerals.

Structures occurring in nature have been replicated to obtain precise control of parameters which produce artificial SH surfaces [18-21]. The lotus leaf would be the best example of a SH texture to be inspired from the nature owing to hierarchical surface

topography with waxy content [9, 18, 20, 21]. One of the developed strategies encouraged by nature involves the functionalization of the particle surface via substitution of reactive groups, for example silanols, with mono- or multifunctional silanes [7, 22-26]. Specifically, fluoroalkyl-modification of a surface has been shown to be a reliable approach both for adequate surface coverage of desired functional groups and for fulfilling the required conditions of low-surface energy as well as protecting high specific surface area of target particles such as silica [7, 27]. Surfaces fabricated through these materials have some practical applications covering chromatographic process, biomedical devices, corrosion-resistant surfaces, self-cleaning, anti-icing and so-forth [18, 24, 28-31]. Nevertheless, some new methodologies involving nonwetting by water and many other liquids have also been the subject of various research [17, 32-35].

Among thousands of forms of algae, a unique group, the diatoms or diatomaceous are able to absorb miscible silica from water at extremely low concentrations and metabolize and accumulate it as an external skeleton which results in sedimentation of diatomaceous earth (DE) on the bottom of a sea or lake [21, 36-38]. The distinguished characteristic of DE is its siliceous skeleton that is a marvel of sophisticated architecture extending to molecular dimensions [21, 36]. To date, DE, therefore, has become a model of many research works associated with biomimetic and nanoscale self-assembly [21, 39, 40]. The prominent example was introduced by Simpson and D'Urso with the concept of superhydrophobic powder via surface coated DE [9]. However, although extensive studies have been carried out on the use of DE powder to make superhydrophobic particles, no single study exists which adequately defines the conditions that can be applicable to any natural powders to make a superhydrophobic surface.

The rationale for the present work is that little is known about various issues corresponding to surface modification of unprocessed natural powders which can have a

significant effect their performance. For example, silica content can vary widely on the mineral type. While reported silica content of typical DE is about 86%, this value could be less than 70% in any other mineral such as talc. Moreover, grafting density is another parameter which was assumed maximal 4 μmol/m^2 for the precipitated silica [7]. Silane structure and functionality degree (i.e., mono-, or multi-functional) are other factors that affect the wetting characteristics. We hypothesize that surface modification of DE can be a model to develop a strategy which then can be applicable to any other unprocessed minerals such as talc to make it superhydrophobic. The proof-of-our principle is based on monitoring the frontiers of water affinity of inherent texture. One-factor-at-a-time method is also preferred to see the influence of every step which can be combined to evaluate the synergistic effects of several factors. Additionally, this is the first study to undertake the likelihood of fabricating tunable SH surface wettability of diatomaceous earth in a controlled way. For the present work, different chlorosilanes were chosen to treat the target surface, with alterations in both reaction conditions and silane structures. The effects of grafting density on water affinity, wettability as well as suitability for nonwetting surface are discussed. The present study fills a gap in the literature by proposing the possibility of potential synergistic approach to be implemented to any proper inherent texture for the production of SH powders.

2. Experimental Section

2.1. Materials

DE mineral (148.62 m^2/g surface area) was provided from Beg-Tug Mineral Company (Ankara/Turkey). Talc mineral (Omyatalc® 5 EXTRA-KS, 23.62 m^2/g surface

area) was supplied by Omya Mining Co. Inc. (Istanbul, Turkey). Silane reagents, demonstrated in Figure 1, 11-(chlorodimethylsilylmethyl)tricosane (Methyltricosane monochlorosilane or Mtcos-MCS); 1.2-Bis(trichlorosilyl)decane (Deca-BisTCS); Ethyldimethylchlorosilane (Ethyl-MCS); n-butyldimetylchlorosilane (nBut-MCS); dodecyldimethylchlorosilane (Dodec-MCS); Nonafluorohexyldimethylchlorosilane (FHex-MCS); Dimethylchlorosilaneperfluorooctyl (PFOct-MCS) and perfluorodecyl-1H,1H,2H,2H-dimetylchlorosilane (PFDec-MCS) were purchased from Gelest Inc. Reagent grade chloroform, hexane and dichloromethane were purchased from Sigma-Aldrich.

2.2. Synthesis of Superhydrophobic Diatomaceous Earth

Step 1 (Without pre-treatment). Two grams of DE "as received" were suspended in 60 ml chloroform in 250 ml round-bottom flask. 0.430 ml of PFDec-MCS was dispersed in 20 ml chloroform, assuming to graft 5 μmol/m^2, and dropwise added to round-bottom flask while the solution was allowed to stir and reflux for 3 h. After DE particles were recovered by filtering at room temperature under vacuum, they were purified by extracting three times in equal volume of hexane and dichloromethane, respectively, to ensure the elimination of any noncovalently bound chloro-functional silane derivatives and other surface impurities. After extraction procedure, the DE particles were collected, taken to vials, and dried at room temperature for 1 day.

Step 2 (Calcination used). Unlike the first step, two grams of two DE samples, calcinated at 400 ^oC, were suspended in 60 ml chloroform in different reaction flasks. 0.430 ml and 0.860 ml of PFDec-MCS were dispersed in 20 ml chloroform and then dropwise added to DE suspension under reflux with stirring, assuming to obtain 5 μmol/m^2 and 10 μmol/m^2 surface coverage, respectively. The reaction process was pursued as described in step 1.

Step 3 (Different Grafting Densities used). The third step for the functionalization of DE surface was analogous to the second step with the only difference being the surface grafting densities. In this case, 0.213 ml and 0.640 ml of PFDec-MCS were used to attain 2.5 μmol/m^2 and 7.5 μmol/m^2 surface coverage. The reaction procedure was identical to step 1.

Step 4 (Various silanes used). In this step, several silane derivatives, which are in turn 0.520 ml of Mtcos-MCS, 0.580 ml of Deca-BisTCS, 0.304 ml of nBut-MCS, 0.246 ml of Ethyl-MCS, 0.536 ml of Dodec-MCS, 0.530 ml of PFOct-MCS, 0.568 ml of FHex-MCS, were used to reach 7.5 μmol/m^2 surface coverage for the DE specimens calcinated at 400 ^oC. The reaction procedures were then continued as described in step 1.

Step 5 (Different mineral used). Two grams of two talc samples, calcinated at 400 ^oC, were used instead of DE. 0.085 ml and 0.113 ml of PFDec-MCS was preferred to achieve the surface coverage of 7.5 μmol/m^2 and 10 μmol/m^2, respectively. All following steps were analogous to step 1.

All the silane treatment steps employed, and abbreviations of the samples and grafting densities are summarized in Table 1.

2.3. Characterization of Samples

2.3.1. Chemical Properties of Samples

The chemical content analysis of "as received" and calcinated DE and Talc were performed by Thermo Scientific ARL Advant'x X-ray fluorescence Spectrometer. Chemical composition of the surface of the samples was analyzed with K-Alpha™$^+$ X-ray Photoelectron Spectrometer (XPS) System. Thermogravimetric analysis of samples was examined with PerkinElmer STA8000. Samples were heated to 1000 ^oC at 10 ^oC/min under the controlled atmosphere (N_2 gas). The percent weight lost up to 1000 ^oC was used to evaluate thermal stability of grafted layers and to predict the grafting density of customized DE.

2.3.2. Morphology Analysis

The surface morphology and microstructure of both “as received” and calcinated DE minerals were studied by using Zeiss EVO 40 Field Emission Scanning Electron Microscopy (FESEM). The materials were introduced onto a conductive carbon tape and coated with gold to prevent charging.

2.3.3. Physical Properties of Samples

Particle size distribution of minerals was determined via Malvern-Mastersizer Hydro2000S in aqueous phase. The Brunauer-Emmett-Teller (BET) surface area of particles was determined by nitrogen adsorption by using Quantachrome NOVA 2000e adsorption instrument after degassing of samples at 150 ^{o}C for 6 h. KSV Attension Theta Lite Optical Tensiometer was used for static and dynamic contact angle measurements. The static measurements were performed by dispensing a water droplet with an average volume of 4 μL whilst dynamic contact angle measurements were employed with different parameters.

2.3.4. Water Affinity Measurements

In order to examine the affinities of HME-blank, HME-2 and HME-3 to water, the following steps have been taken: All materials were suspended in chloroform and ultrasonicated for 1 h in order for X materials to be dispersed thoroughly in solvent. Then, the solutions were kept at room temperature for 24 h. By using a shadow mask, gold electrodes with 100 nm thickness, 17 μm gap and width of 1500 μm were evaporated thermally on the glass substrates. In order to form thin films of each material, 2 μL of each solution was drop casted between the gold electrodes as depicted in Figure S1 of supporting information. After preparation of thin films of each material, the experimental setup consisting of 2-channel gas flow system with required software and equipment was used (Supporting Information, Figure S2). Mass flow meters (MFCs) control the system at flows ranging between 0 and 1000 sccm and send the flow of pure inert nitrogen (dry N_2) into water bubbler to produce wet nitrogen

(wet N_2). A commercial humidity sensor (Sensirion, Switzerland) and a sourcemeter (Keithley, model 2636A, USA) were synchronously used to record the real-time humidity and electrical response, respectively. Water affinities of HME-blank, HME-2 and HME-3 were investigated by exposing prepared samples to 86% RH at room temperature and measuring the change in the electrical response due to water adsorption.

3. Results and Discussion

Since the present study was designed to develop a model work for natural powders with low surface energy and to achieve a desired degree of superhydrophobicity in a controlled manner, the surface modification conditions were optimized to produce enhanced surface coverage on DE. The obtained conditions were taken as model work and applied to Talc mineral, which was preferentially chosen due to the fact that it has peculiar affinity toward water. The methodology based on the chemical content, morphological character and physical properties of chosen powders are the key aspects to maximize grafting density. In this respect, the following results highlight several fundamental features of the inherent textures mentioned above.

The chemical composition, surface area and particle size data of the “as-received” DE are given in Table S1. The content of silicon oxide was found to be 65.5% for crude DE which is less than the typical silica content of reported crude DE [9].

The step 1 was employed to oversimplify substitution of silanols with fluorocarbon substituents. In previous studies,[9, 21] preference of crude (uncalcinated) DE has been

reported for the synthesis superhydrophobic powders. By contrast, samples recovered from the first step (HME-1) have not fulfilled the required conditions for hydrophobicity. Note, however, that in order to be suitable for the silylation of any surface of silica based particle, it is essential for the SAM precursor to contact and bind to the particle surface without confronting any obstacle [9, 41]. It can be deduced that chemical contaminants like organic impurities and absorbed water have more profound effects for the samples with low percent silica content compared to that of the reported counterparts.

The use of gradual calcination studies were performed, in which the change in percent silica content, particle size and surface area were screened according to various calcination temperatures in an attempt to optimize reaction conditions (See Supporting Information of Table S1). In agreement with previous reports,[9] calcination can be performed to eliminate organic contaminants and physically adsorbed water that can occupy the active features of the DE and interfere with the bonding of the SAM precursor to the DE surface. Table S1 shows the XRF, BET and particle size results of DE minerals calcinated at different temperatures. As seen in Table S1, the amount of silica (SiO_2) and other oxide compounds increased with an increase of calcination temperatures whilst the surface area decreases. It's known that customization of the surface to load hydrophobicity entails keeping high specific surface area and excess amount of active features such as silica with eliminated contaminantsand physisorbed water. In light of this information and recent studies,[22-24] DE calcinated at 400 ^{o}C was considered to be the best conditions to fulfill the desired requirements (For SEM micrographs of DE particles, see Figure S4 of the Supporting Information).

For the practice of efficacy of calcination on the surface modification of DE particles, the grafting procedure described in step 2 has been followed. Herein, the effect of grafting density on the water affinity of the diatomaceous has also been investigated. As specified before, the object is to see what happens when DE is functionalized with silane moieties with

increasing grafting density in terms of water affinity. Hence, thin films of these DE based specimens were readily developed on the surface of gold electrodes separated with a 3 μm gap to compare the electrical properties of them in the presence of water molecules. As seen in Figure 2, depicting adsorption and desorption characteristics of each material, the red, blue and green dashed lines represent the variations in the resistance of HME-blank, HME-2 and HME-3, respectively. The electrodes coated with these materials measured changes in the resistance due to adsorption and desorption of water vapour. The real-time relative humidity (RH) values in the test cell were simultaneously collected with a commercial Sensirion sensor during measurements. This sensor displayed 15% RH when the test cell was purged with dry N_2 while it became 86% RH with only wet N_2 (obtained by sending dry N_2 through a water bubbler kept at a constant room temperature). Dry and wet N_2 was used consecutively in 200 s periods in order to investigate the affinity of each electrode to water during adsorption process. When fully dry nitrogen was sent to the test cell, the maximum resistances of each material (R_0) have been obtained as 2.47×10^8 Ω, 2.40×10^8 Ω and 2.38×10^8 Ω, respectively. The water affinity of each material has been defined as ($\Delta R/R_0$), where R_0 is initial (maximum) resistance of the film and ΔR is the change in the resistance of the film[42]. The maximum response of each material has been found as 102.4%, 99.7% and 95.9%, respectively. As a consequence of the increase in the RH giving rise to an increase in the amount of adsorbed or capillary-condensed water molecules, the resistances of thin films of each material have decreased according to the experimental results. It has also been seen that the HME-blank has performed the highest affinity towards water molecules while this affinity has decreased as grafting density increased, leading us to consider that varying the grafting density could be the key parameter to tune the hydrophobic characteristic of relevant diatomaceous.

To assess whether and how tunable hydrophobic surface are produced, DE powders were subjected to the grafting procedure defined in step 3. Grafting densities were rendered between the values indicated in step 2 to get more reliable results. In an attempt to optimize the analysis parameters and to evaluate a correlation between them, a comparative screening study was carried out. The data of the samples gathered from step 2 and step 3 were synergistically examined as well as their results from TGA weight loss, BET surface area, and contact angle measurements which are detailed in Table 2. It is significant to note that in addition to the surface coverage estimation from TGA analysis, a strong correlation between BET "C constant" and surface energy has previously been reported in the literature.[7, 43-46] The required features of hydrophobic materials are a low content of hydrophilic group due to high grafting density (as represented by TGA weight loss), and a low surface energy (a low BET "C constant") giving rise to high contact angle. Therefore it is concluded that, for the samples with a high amount of fluoroalkyl grafting density on the particle surface, the higher the amount of percent weight loss in TGA will be and the lower the surface energy (the lower BET "C constant") leading to gradual increase in static contact angle. A high specific surface area is another desired condition for surfaces to be liquid repellent as it demonstrates protection of multiscale surface roughness that is favorable for creating a solid-liquid-air interface. Nevertheless, the degree to which the surface area is altered during the concerted silane substitution is uncertain; however, it is anticipated to be as great as or lower than the "blank" sample.[7]

According to Table 2, Figure 3 a, b and Figure 4, the HME-Blank underwent a modest 8.20 % weight loss due to desorption of strongly bonded species or condensation of silanols, whereas percent weight loss gradually increases up to 18.92% in HME-3 owing to an increase in grafting density. This increase was also confirmed by the gradual decrease in BET "C constant" which proves that decreasing the surface energy increases the grafting density.

Moreover, it is apparent from Figure 3b that there is a decrease in the increment of percent weight loss differences between the samples from HME-blank to HME-3. It is postulated that the surface of the DE particles started to saturate with an increase in grafting density and steric hindrance became more prominent due to the saturation. Specifically, a slight difference in percent weight loss between HME-4 and HME-3 is the most meaningful indicator of saturation. Further, this phenomenon is proved by the contact angle measurements that follow the same trend. The decrease in the rise of contact angle differences between the samples from HME-blank to HME-3 is attributed to a drop in the amount of free silanols on the surface of the particles, which bring about increasing wettability (for additional evaluation of surface modification, Figure S3a, b of Supporting Information can be seen) .

Other eligibility criteria of superhydrophobicity of particles are defined as having both contact angle hysteresis (CAH) and sliding angle (SA) < 10 [10, 12]. Dynamic contact angle analysis was carried out with water droplets by using both sliding (measurement on a slope) and extension-contraction methods (0,2 µL/s step increase and decrease) for different materials. As expected, “as received” DE and HME-Blank samples are completely wet. Nevertheless, HME-5 and HME-2 displayed inconclusive results during dynamic experiments. This is a consequence of low surface energy of DE particles during the addition of a water droplet on the functionalized DE surface that caused loosely adhered DE particles to come off the glass substrate and accumulate around/into the water beads. In some circumstances, water beads reached and wetted the surface of glass substrate. In agreement with the literature, this behavior is understandable in light of the study on ‘‘liquid marbles’’ in which droplets of ionic liquid or high surface tension water are efficiently coated by particles having a low surface energy such as sub-micrometer oligomeric tetrafluoroethylene (OTFE) particles or hydrophobized silica.[47, 48] However, HME-4 and HME-3 did not

display such unwanted behavior but instead they demonstrated strong adhesion with the glass substrate enabling measurement of dynamic contact angle. For the former one, the sliding technique (with a tilted angle of 7^{o}) was carried out to measure the advancing-receding contact angles and the result is given in Figure 5a. The surface resulted in $\theta_{adv}/\theta_{rec}$ = 166.52/139.71 (CAH≈ 26.81). A large water bead stuck to substrate surface even with a tilt angle of 90^{o} as seen in Figure 5b. The result obtained from sliding method was also confirmed with extension-contraction method, which gave rise to $\theta_{adv}/\theta_{rec}$ = 166.17/139.98 (CAH≈ 26.19) (see Figure 5c and d). A high contact angle hysteresis and a large water droplet stuck to substrate are indicators of a rough surface with complete wetting between the droplet and interface of the surface. For the latter one, a sliding method could not be used due to the fact that water beads rolled off the surface with even quite low tilt angle such that the measurement of a dynamic contact angle on an inclined surface (7^{o} tilt angle) via dispensing 10 µL droplet was not possible as the droplet spontaneously rolled off the surface (Video S1). To stabilize the water bead on the surface, both tilt angle and water droplet volume were decreased to 4^{o} and 3.5 µL, respectively. Interestingly, the droplet did not dispense on the surface even though dispenser of the tensiometer was triggered several times (Video S2). As a final trial, the tilt angle and droplet volume were kept constant (4^{o}, 3.5 µL) but the distance between the surface and dispenser was increased 2-fold. The droplet was seen rolling off the surface (Video S3). Therefore the extension-contraction method was preferred on a horizontal surface of HME-3 to conduct dynamic contact angle measurement. The surface resulted in $\theta_{adv}/\theta_{rec}$ = 166.15/165.38 (CAH≈ 0.77) (see Figure 6a, b). This result is consistent with highly silylated and homogeneous surface with extensive fluoroalkyl content.

Additional insight into low surface energy particles has been gained by varying silane structures and degree of functionality. Chloro-functional silanes were preferentially used over the alkoxy-functional silanes since previous studies have emphasized the importance of using

chlorosilanes for direct substitution with surface silanols in the absence of water [7, 49]. However, excess amount of surface water has regularly been observed to contribute to silanols substitution via chloro- or alkoxy-functional groups [50-52] surface customization by grafting silanes in anhydrous conditions. This effect ought to minimize self-condensation of hydrolyzed silane agents that result in undesired side products [53, 54]. Another additional case reported in the literature is associated with the superiority of monochlorosilanes over multifunctional analogues in terms of producing a homogeneous monolayer with a lower silanols content as well as having the better water repellent character for precipitate silica [7]. Although the surface of DE is more similar in composition to that of precipitated silica [9] monochlorosilane was utilized in between step 1-3 to investigate the effects of the aforementioned factors as well as in step 4 to explore the influence of the chain length and several silane structures. The silane modifiers were chosen according to their availability and the desire to maximize the sorts of silane structures.

Further exploration of the key features of DE particles with respect to changing silane structures is examined in Step 4. For the samples grafted with fluoroalkyl silanes (PFDec-MCS, PFOct-MCS and FHex-MCS), the contact angles undergo gradual decrease with decreasing chain length, indicating that the longer the fluoroalkyl chain length is, the higher the hydrophobicity that causes a gradual decrease in the surface energy (See Figure 7a-c). In accordance with the present result, the previous work has indicated that increasing fluoroalkyl chain length causes remarkable decrease in BET “C constant”, which also proves the lower surface energy and provides additional explanation for gradual decrease of contact angles [7]. For the elaboration of the effect of silane structures, DE particles were grafted with silane with a long alkyl chain. In this case, the hydrophobic features of Dodec-MCS (Figure 7d) is comparable to water-repellency properties obtained with the most fluorinated silane (PFDec-MCS). This finding is rather favorable from ecotoxic approach because recent

studies revealed the persistence and bioaccumulation potential of fluorinated alkyl substances, which is the key challenge for bio inspired materials.[55-59] Compared with the fluoroalkyl chain, there is a considerable decrease in the contact angle with decreasing hydrocarbon chain length as expected (Figure 7e, f).

Another comparative screening study concerning hydrophobicity was conducted to elucidate the effect of chain variation and degree of functionality of silane substances. Compared to Dodec-MCS, Mtcos-MCS displayed wettable characteristics in spite of having a branched and long hydrocarbon chain (Figure 8a). This result may be explained by the fact that the bulky structure of the used silane makes steric effects more dominant and inhibits its reaction that gives rise to remaining much of the silanols without substitution and significantly increased heterogeneity. As to Deca-BisTCS, it displayed higher hydrophilicity with respect to Dodec-MCS (Figure 8b). This result is in accord with recent literature [7] indicating that multifunctional silane treatment causes a higher amount of silanols to remain.

Taken together, preparation conditions of inherent texture, ideal grafting density and reaction conditions have been optimized and applied to talc as depicted in step 5. Talc mineral, preferred on account of peculiar affinity towards water, performs either hydrophilic or hydrophobic behavior depending on relative humidity.[60] This dichotomy has been overcome through grafting the talc surface that has given rise to permanent water repellency. It is possible to state that the hypothesis posed at the beginning is confirmed by the findings indicated here i.e. that the static water contact angles of the samples were found to be in turn 165^{o} and 166^{o} as depicted in Figure 9a, b. For the talc surface with grafting density of 10 μmol/m^{2}, the surface resulted in $\theta_{adv}/\theta_{rec}$ = 159.25^{o} /138.68^{o} (CAH≈ 20.57) by sliding method (Figure 10). In addition to high contact angle hysteresis, the water bead was also attached to the surface at any tilt angle ranging between 0^{o} and 90^{o}. These are considered to stem from

the rough surface with complete wetting between the water bead and surface interface, which may be attributed to Wenzel's model describing homogeneous wetting regime.[10, 61]

4. Conclusion

Fluorocarbon-functional silanes were found to be the most effective modifiers to attain superhydrophobicity on surfaces of natural texture by comparison to hydrocarbon-functional silanes. The chemical content of the crude and calcinated minerals were investigated via XRF technique whereas the covalent attachment of silanes was illusidated by XPS method. Water affinity data of surface grafted particles showed that surface silanols were treatable to reach tunable wettability and to optimize grafting methodology. It can also be deduced that the proposed methodology could pave the way to be applied to other natural textures such as talc. According to thermogravimetric analysis, used to investigate grafting density, it can be concluded that as the amount of fluoroalkyl grafting density on the particle surface increased, the amount of percent weight loss in TGA is augmented. This phenomenon was also proven by both BET analysis and static contact angle measurements i.e. anincrease in grafting density gave rise to a decrease in the BET "C constant" (lower surface energy) which also led to a gradual increase in the static contact angle. The treatment with monofunctional chlorosilanes was found to provide better superhydrophobic properties than their multifunctional counterparts. Dynamic contact angle measurements resulted in low contact angle hysteresis and it was observed that the water bead rolled off the surface even with a small droplet volume at very low tilt angle for DE samples. However, as for talc, the water bead was attached to the surface at any tilt angle ranging between 0^o and 90^o and caused high contact angle hysteresis. This result is considered to be due to the rough surface with complete wetting between the water droplet and surface interface, which might be related to Wenzel's model describing a homogeneous wetting regime. This study offers important

insights into producing superhydrophobic surfaces and potential synergistic approach to be implemented to any proper inherent texture for the production of SH powders.

Figures

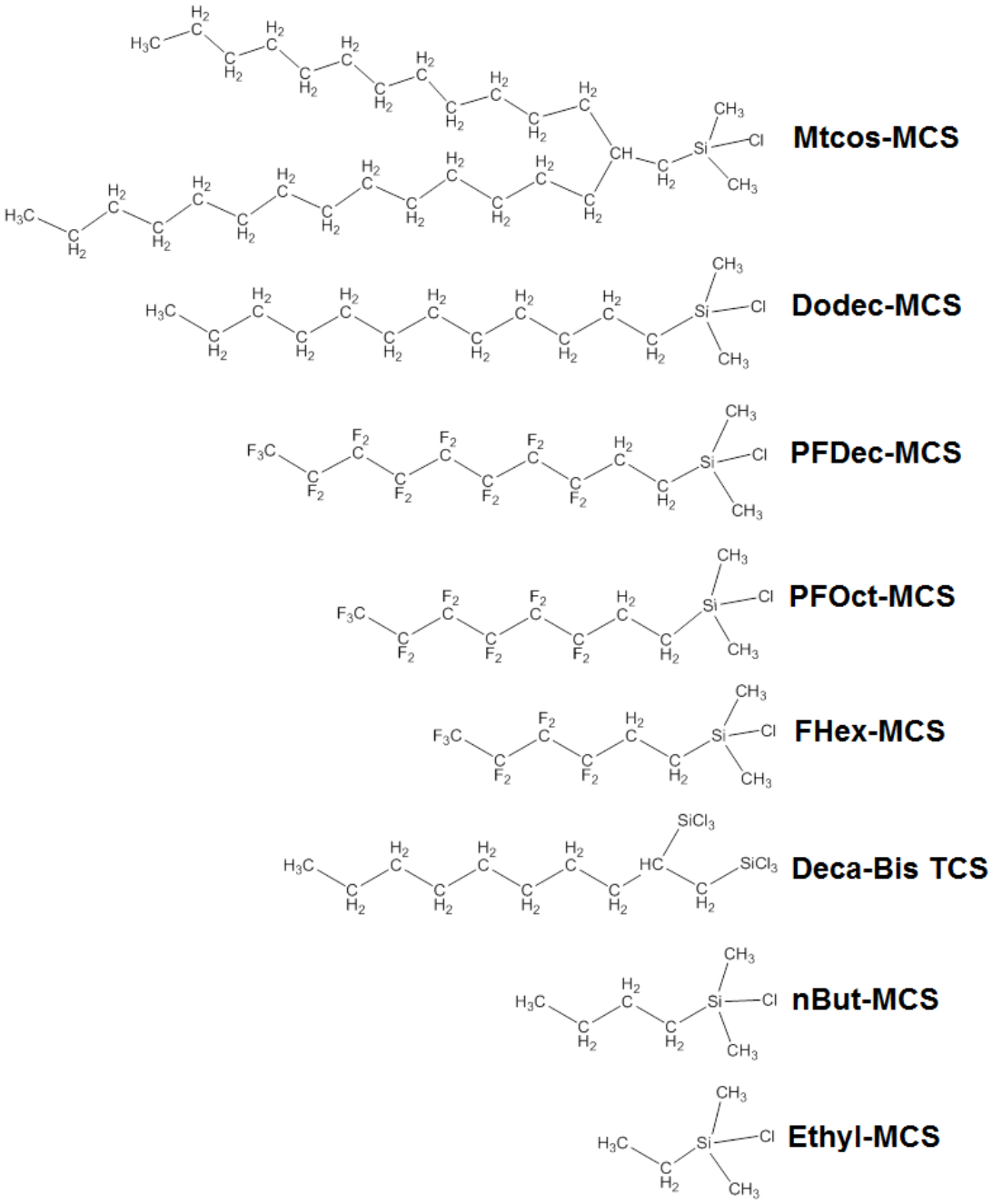

Figure 1. Silane modifiers used in this work

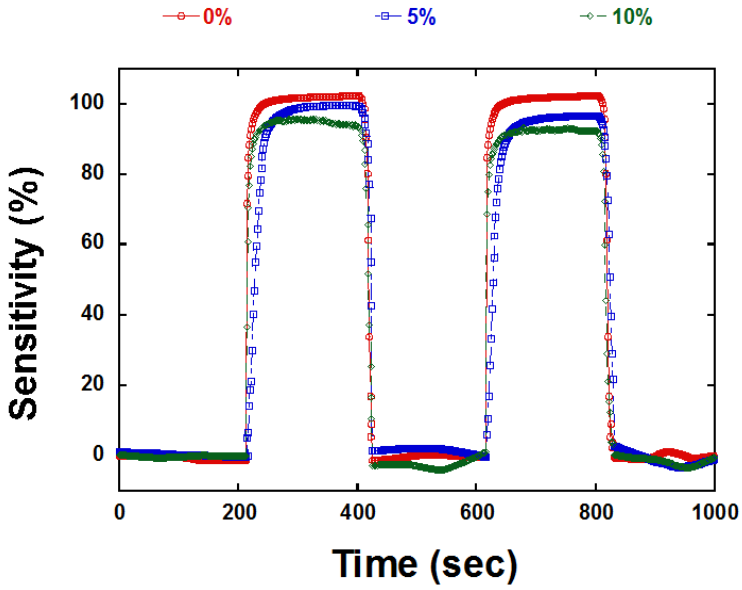

Figure 2. Effect of Grafting Density on Water Affinity of Samples

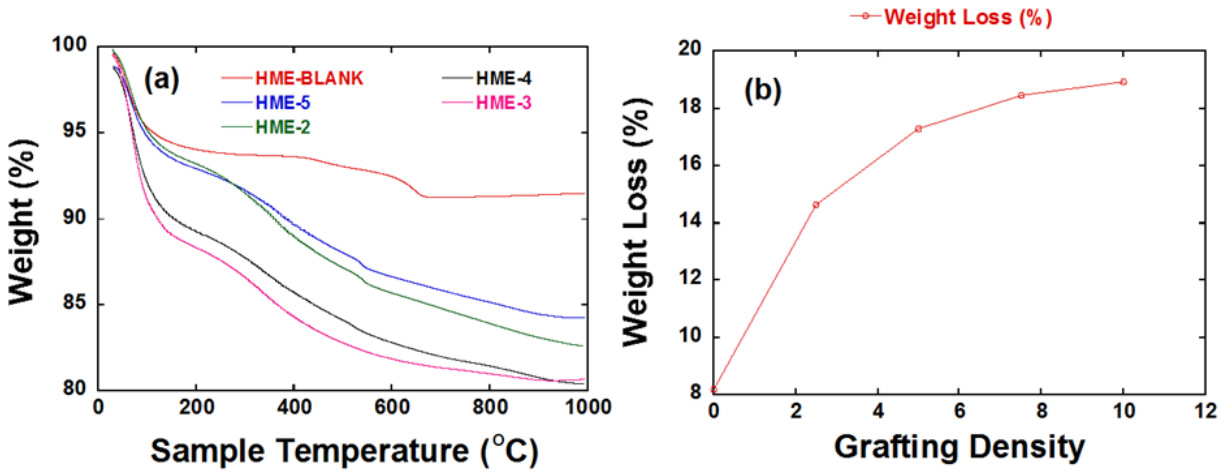

Figure 3. a) TGA Thermograms of PFOct-MCS grafted samples, b) Effect of PFOct-MCS grafting Density on TGA Weight Loss

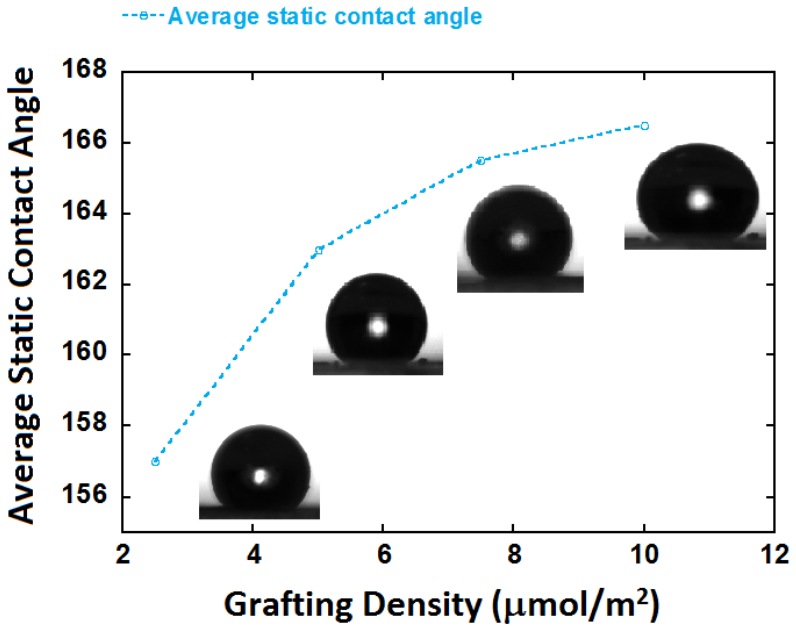

Figure 4. Effect of Grafting Density on Average Static Contact Angle

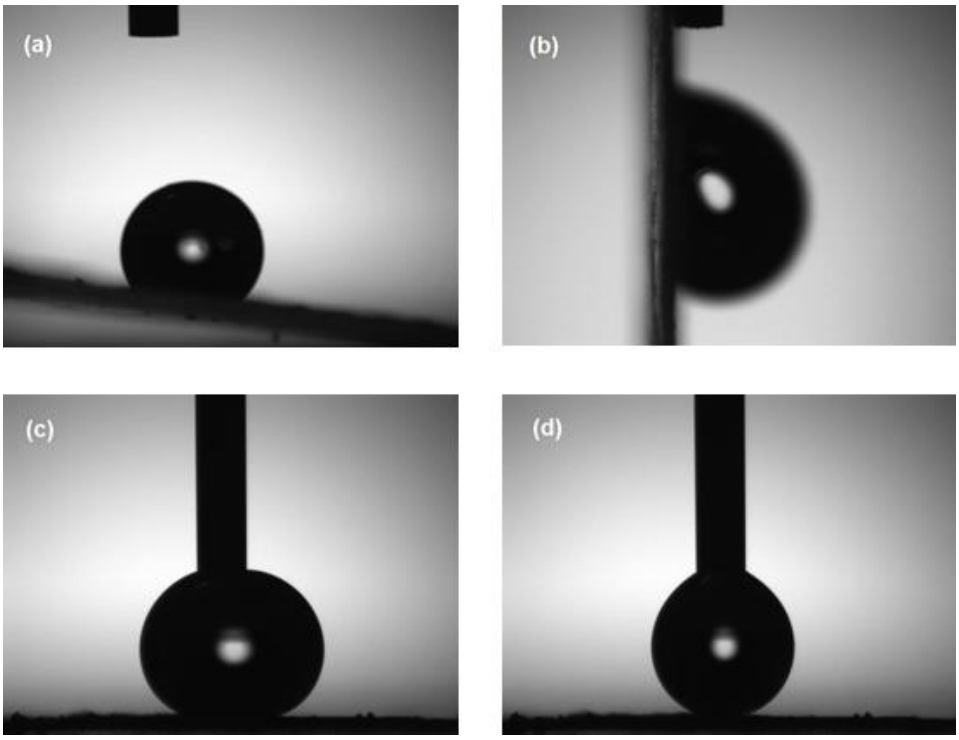

Figure 5. Shape of Water Droplets Illustrating Wetting Behaviour of HME-4 a) Inclined Surface for Advancing and Receding Contact Angles, b) 10 µl of Water Droplet Pinned to the Surface of HME-4, c) Water Droplet Extended to 5 µl for Advancing Contact Angle, d) Water Droplet Contracted to 4 µl for Receding Contact Angle

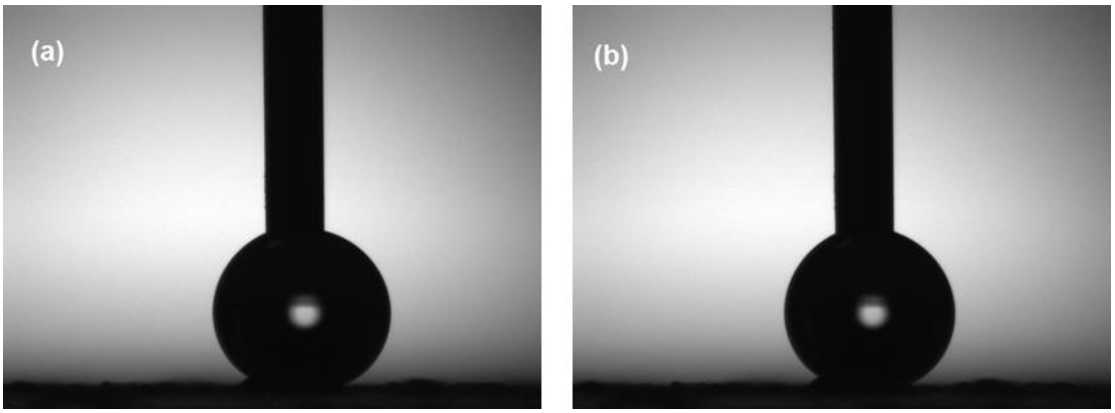

Figure 6. Shape of Water Droplets Illustrating Wetting Behaviour of HME-3 a) Water Droplet Extended to 5 µl for Advancing Contact Angle, b) Water Droplet Contracted to 4 µl for Receding Contact Angle

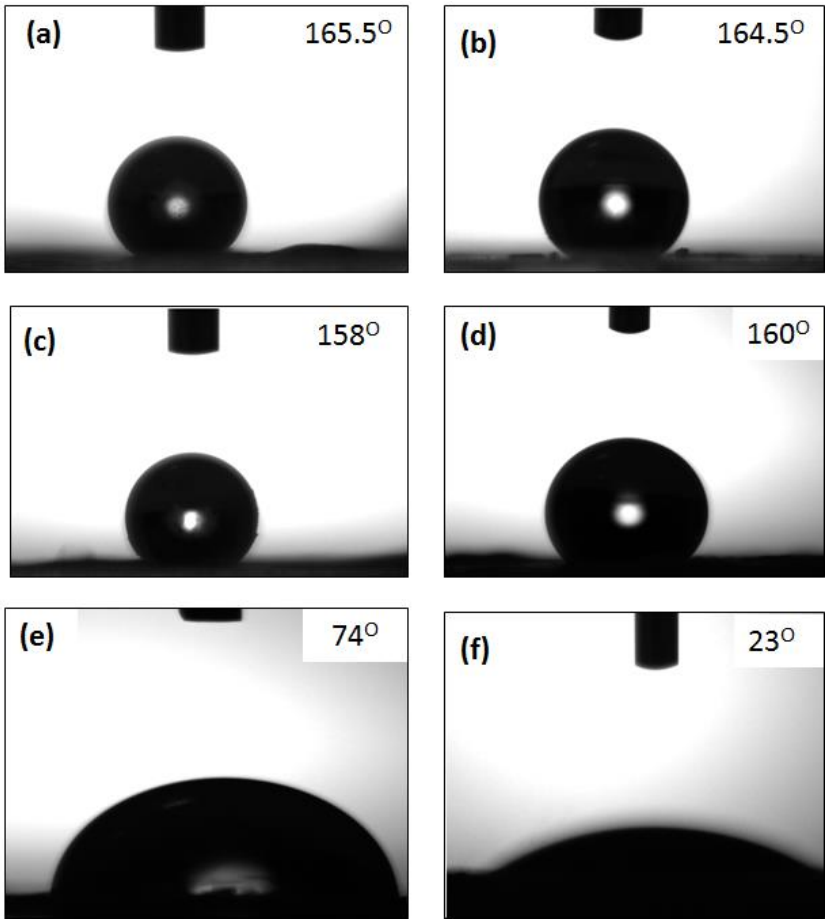

Figure 7. Changes in Water Contact Angle with regards to Different Silane Structures a) PFDec-MCS Modified DE (HME-4), b) PFOct-MCS Modified DE (HME-6), c) FHex-MCS Modified DE (HME-7), d) Dodec-MCS Modified DE (HME-10), e) nBut-MCS Modified DE (HME-8), f) Ethyl-MCS Modified DE (HME-9)

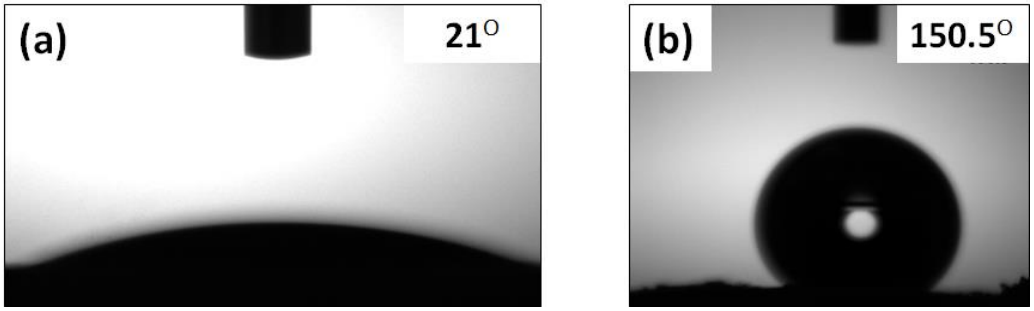

Figure 8. a) Effect of Chain Variation on Water Contact Angle (HME-9), b) Effect of Degree of Functionality on Water Contact Angle (HME-12)

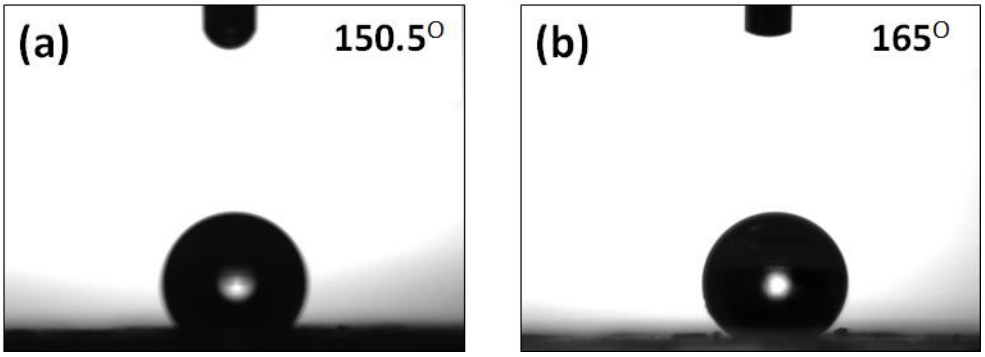

Figure 9. Water Contact Angles of PFDec-MCS Modified TALC a) HME-13, b) HME-14

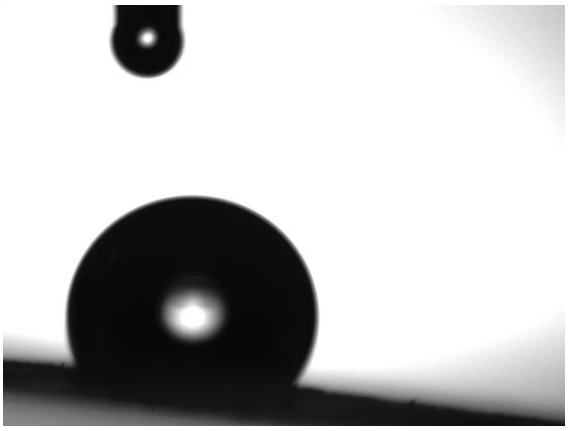

Figure 10. Dynamic Contact Angle Measurement of HME-14

Tables

Table 1. Summary of Surface Functionalized Minerals

Sample	Mineral	Calcination (°C)	Silane	Grafting Density (μmol/m^2)	Step
HME-Bare	DE	None	None	None	-
HME-Blank	DE	400	None	None	-
HME-1	DE	None	PFDec-MCS	5	1
HME-2	DE	400	PFDec-MCS	5	2
HME-3	DE	400	PFDec-MCS	10	2
HME-4	DE	400	PFDec-MCS	7.5	3
HME-5	DE	400	PFDec-MCS	2.5	3
HME-6	DE	400	PFOct-MCS	7.5	4
HME-7	DE	400	FHex-MCS	7.5	4
HME-8	DE	400	nBut-MCS	7.5	4
HME-9	DE	400	Ethyl-MCS	7.5	4
HME-10	DE	400	Dodec-MCS	7.5	4
HME-11	DE	400	Mtcos-MCS	7.5	4
HME-12	DE	400	Deca-BisTCS	7.5	4
HME-13	TALC	400	PFDec-MCS	7.5	5
HME-14	TALC	400	PFDec-MCS	10	5

Table 2. Influence of Reaction Parameters on Key Features of Treated DE Samples

Sample	Grafting Density (μmol/m^2)	% Weight Loss	BET "C constant"	BET Area m^2/g	Contact angle
HME-Blank	None	8.20	146	117	Wet
HME-5	2.5	14.64	35	119	157°
HME-2	5.0	17.29	25	86	163°
HME-4	7.5	18.45	24	109	165.5°
HME-3	10.0	18.92	21	83	166.5°

Associated Content

Supporting Information. Additional figures, tables, videos, and discussion. This material is available free of charge via the internet http://pubs.acs.org.

Author Contributions

The manuscript was written through contributions of all authors. All authors have given approval to the final version of the manuscript.

Acknowledgement

We gratefully acknowledge the Izmir Katip Celebi University, Scientific Research Foundation for financial support of this study.

References

[1] Zhang, X.; Shi, F.; Niu, J.; Jiang, Y. G.; Wang, Z. Q. Superhydrophobic surfaces: from structural control to functional application. *J Mater Chem* **2008,** *18* (6), 621-633.

[2] Gao, L. C.; McCarthy, T. J.; Zhang, X. Wetting and Superhydrophobicity. *Langmuir* **2009,** *25* (24), 14100-14104.

[3] Roach, P.; Shirtcliffe, N. J.; Newton, M. I. Progess in superhydrophobic surface development. *Soft Matter* **2008,** *4* (2), 224-240.

[4] Feng, X. J.; Jiang, L. Design and creation of superwetting/antiwetting surfaces. *Adv Mater* **2006,** *18* (23), 3063-3078.

[5] Nosonovsky, M.; Bhushan, B. Superhydrophobic surfaces and emerging applications: Non-adhesion, energy, green engineering. *Curr Opin Colloid In* **2009,** *14* (4), 270-280.

[6] Chhatre, S. S.; Choi, W.; Tuteja, A.; Park, K. C.; Mabry, J. M.; McKinley, G. H.; Cohen, R. E. Scale Dependence of Omniphobic Mesh Surfaces. *Langmuir* **2010,** *26* (6), 4027-4035.

[7] Campos, R.; Guenthner, A. J.; Haddad, T. S.; Mabry, J. M. Fluoroalkyl-Functionalized Silica Particles: Synthesis, Characterization, and Wetting Characteristics. *Langmuir* **2011,** *27* (16), 10206-10215.

[8] Polizos, G.; Winter, K.; Lance, M. J.; Meyer, H. M.; Armstrong, B. L.; Schaeffer, D. A.; Simpson, J. T.; Hunter, S. R.; Datskos, P. G. Scalable superhydrophobic coatings based on fluorinated diatomaceous earth: Abrasion resistance versus particle geometry. *Appl Surf Sci* **2014,** *292*, 563-569.

[9] Simpson, J. T.; D'Urso, B. R. Superhydrophobic diatomaceous earth. Google Patents, 2012.

[10] Ebert, D.; Bhushan, B. Transparent, Superhydrophobic, and Wear-Resistant Coatings on Glass and Polymer Substrates Using SiO2, ZnO, and ITO Nanoparticles. *Langmuir* **2012,** *28* (31), 11391-11399.

[11] Holmberg, K.; Jonsson, B.; Kronberg, B.; Lindman, B. Surfactants and Polymers in Aqueous Solution. Copyright. John Wiley & Sons, Ltd. ISBN: 0-471-49883-1, 2002.

[12] Ogihara, H.; Xie, J.; Okagaki, J.; Saji, T. Simple Method for Preparing Superhydrophobic Paper: Spray-Deposited Hydrophobic Silica Nanoparticle Coatings Exhibit High Water-Repellency and Transparency. *Langmuir* **2012,** *28* (10), 4605-4608.

[13] Guo, M.; Ding, B.; Li, X. H.; Wang, X. L.; Yu, J. Y.; Wang, M. R. Amphiphobic Nanofibrous Silica Mats with Flexible and High-Heat-Resistant Properties. *J Phys Chem C* **2010,** *114* (2), 916-921.

[14] Kumar, R. T. R.; Mogensen, K. B.; Boggild, P. Simple Approach to Superamphiphobic Overhanging Silicon Nanostructures. *J Phys Chem C* **2010,** *114* (7), 2936-2940.

[15] Li, H. J.; Wang, X. B.; Song, Y. L.; Liu, Y. Q.; Li, Q. S.; Jiang, L.; Zhu, D. B. Super-"amphiphobic" aligned carbon nanotube films. *Angew Chem Int Edit* **2001,** *40* (9), 1743-1746.

[16] Darmanin, T.; Guittard, F. One-pot method for build-up nanoporous super oil-repellent films. *J Colloid Interf Sci* **2009,** *335* (1), 146-149.

[17] Hsieh, C. T.; Wu, F. L.; Chen, W. Y. Superhydrophobicity and superoleophobicity from hierarchical silica sphere stacking layers. *Mater Chem Phys* **2010,** *121* (1-2), 14-21.

[18] Guo, Z. G.; Liu, W. M.; Su, B. L. Superhydrophobic surfaces: From natural to biomimetic to functional. *J Colloid Interf Sci* **2011,** *353* (2), 335-355.

[19] Neinhuis, C.; Barthlott, W. Characterization and distribution of water-repellent, self-cleaning plant surfaces. *Ann Bot-London* **1997,** *79* (6), 667-677.

[20] Barthlott, W.; Neinhuis, C. Purity of the sacred lotus, or escape from contamination in biological surfaces. *Planta* **1997,** *202* (1), 1-8.
[21] Oliveira, N. M.; Reis, R. L.; Mano, J. F. Superhydrophobic Surfaces Engineered Using Diatomaceous Earth. *Acs Appl Mater Inter* **2013,** *5* (10), 4202-4208.
[22] Buszewski, B.; Jezierska, M.; Welniak, M.; Berek, D. Survey and trends in the preparation of chemically bonded silica phases for liquid chromatographic analysis. *Hrc-J High Res Chrom* **1998,** *21* (5), 267-281.
[23] Sayari, A.; Hamoudi, S. Periodic mesoporous silica-based organic - Inorganic nanocomposite materials. *Chem Mater* **2001,** *13* (10), 3151-3168.
[24] Zhang, W. Fluorocarbon stationary phases for liquid chromatography applications. *J Fluorine Chem* **2008,** *129* (10), 910-919.
[25] Pickering, J. Patent 7,252,885. Aug, 2007.
[26] Coggio, W. Patent 7,473,462. Jan, 2009.
[27] Fields, J. T.; Garton, A.; Poliks, M. D. Fluoroalkylsilanes in silica/fluoropolymer composites. *Polymer composites* **1996,** *17* (2), 242-250.
[28] Berendsen, G. E.; Pikaart, K. A.; Galan, L. D.; Olieman, C. "(Heptadecafluorodecyl)Dimethylsilyl Bonded Phase for Reversed-Phase Liquid-Chromatography. *Anal Chem* **1980,** *52* (12), 1990-1993.
[29] Roshchina, T. M.; Shoniya, N. K.; Lagutova, M. S.; Nikol'skaya, A. B.; Borovkov, V. Y.; Kustov, L. M. Adsorption of water, diethyl ether, and acetonitrile on silicas with grafted perfluorohexyl coatings. *Russ J Phys Chem a+* **2009,** *83* (2), 290-297.
[30] Monde, T.; Nakayama, N.; Yano, K.; Yoko, T.; Konakahara, T. Adsorption characteristics of silica gels treated with fluorinated silylation agents. *J Colloid Interf Sci* **1997,** *185* (1), 111-118.
[31] Kamiusuki, T.; Monde, T.; Yano, K.; Yoko, T.; Konakahara, T. Preparation of branched-polyfluoroalkylsilane-coated silica gel columns and their HPLC separation characteristics. *Chromatographia* **1999,** *49* (11-12), 649-656.
[32] Bravo, J.; Zhai, L.; Wu, Z.; Cohen, R. E.; Rubner, M. F. Transparent superhydrophobic films based on silica nanoparticles. *Langmuir* **2007,** *23* (13), 7293-7298.
[33] Xue, L.; Li, J.; Fu, J.; Han, Y. Super-hydrophobicity of silica nanoparticles modified with vinyl groups. *Colloids and Surfaces A: Physicochemical and Engineering Aspects* **2009,** *338* (1), 15-19.
[34] Sheen, Y. C.; Huang, Y. C.; Liao, C. S.; Chou, H. Y.; Chang, F. C. New approach to fabricate an extremely super-amphiphobic surface based on fluorinated silica nanoparticles. *J Polym Sci Pol Phys* **2008,** *46* (18), 1984-1990.
[35] Garcia, N.; Benito, E.; Guzman, J.; Tiemblo, P. Use of p-toluenesulfonic acid for the controlled grafting of alkoxysilanes onto silanol containing surfaces: Preparation of tunable hydrophilic, hydrophobic, and super-hydrophobic silica. *J Am Chem Soc* **2007,** *129* (16), 5052-5060.
[36] Iler, R. K. The chemistry of silica. Wiley, New York, 1979.
[37] Yang, W.; Lopez, P. J.; Rosengarten, G. Diatoms: Self assembled silica nanostructures, and templates for bio/chemical sensors and biomimetic membranes. *Analyst* **2011,** *136* (1), 42-53.
[38] Rabosky, D. L.; Sorhannus, U. Diversity dynamics of marine planktonic diatoms across the Cenozoic. *Nature* **2009,** *457* (7226), 183-186.

[39] Begum, G.; Rana, R. K.; Singh, S.; Satyanarayana, L. Bioinspired Silicification of Functional Materials: Fluorescent Monodisperse Mesostructure Silica Nanospheres. *Chem Mater* **2010,** *22* (2), 551-556.
[40] Fei, B.; Hu, Z. G.; Lu, H. F.; Xin, J. H. Preparation of a panoscopic mimic diatom from a silicon compound. *Small* **2007,** *3* (11), 1921-1926.
[41] Greenwood, P. Surface modifications and applications of aqueous silica sols. Chalmers University of Technology2010.
[42] Liu, L.; Ye, X.; Wu, K.; Han, R.; Zhou, Z.; Cui, T. Humidity sensitivity of multi-walled carbon nanotube networks deposited by dielectrophoresis. *Sensors* **2009,** *9* (3), 1714-1721.
[43] Kazakevich, Y. V.; Fadeev, A. Y. Adsorption characterization of oligo (dimethylsiloxane)-modified silicas: an example of highly hydrophobic surfaces with non-aliphatic architecture. *Langmuir* **2002,** *18* (8), 3117-3122.
[44] Nikoobakht, B.; El-Sayed, M. A. Evidence for bilayer assembly of cationic surfactants on the surface of gold nanorods. *Langmuir* **2001,** *17* (20), 6368-6374.
[45] Wang, Q.; Baker, G. A.; Baker, S. N.; Colón, L. A. Surface confined ionic liquid as a stationary phase for HPLC. *Analyst* **2006,** *131* (9), 1000-1005.
[46] Thomas, M. M.; Clouse, J. A. Thermal analysis of compounds adsorbed on low-surface-area solids: Part 1. measurement and characterization by TGA. *Thermochimica acta* **1989,** *140*, 245-251.
[47] Gao, L.; McCarthy, T. J. Ionic liquid marbles. *Langmuir* **2007,** *23* (21), 10445-10447.
[48] Aussillous, P.; Quere, D. Liquid marbles. *Nature* **2001,** *411* (6840), 924-927.
[49] Tripp, C.; Veregin, R.; Hair, M. Effect of fluoroalkyl substituents on the reaction of alkylchlorosilanes with silica surfaces. *Langmuir* **1993,** *9* (12), 3518-3522.
[50] Fadeev, A. Y.; Kazakevich, Y. V. Covalently attached monolayers of oligo (dimethylsiloxane) s on silica: a siloxane chemistry approach for surface modification. *Langmuir* **2002,** *18* (7), 2665-2672.
[51] Hair, M.; Tripp, C. Alkylchlorosilane reactions at the silica surface. *Colloids and Surfaces A: Physicochemical and Engineering Aspects* **1995,** *105* (1), 95-103.
[52] Blitz, J. P.; Murthy, R. S.; Leyden, D. E. Studies of silylation of Cab-O-Sil with methoxymethylsilanes by diffuse reflectance FTIR spectroscopy. *J Colloid Interf Sci* **1988,** *121* (1), 63-69.
[53] Xu, B.; Vermeulen, N. Preparation of wall-coated open-tubular capillary columns for gas chromatography. *J Chromatogr A* **1988,** *445*, 1-28.
[54] Fadeev, A. Y.; McCarthy, T. J. Self-assembly is not the only reaction possible between alkyltrichlorosilanes and surfaces: monomolecular and oligomeric covalently attached layers of dichloro-and trichloroalkylsilanes on silicon. *Langmuir* **2000,** *16* (18), 7268-7274.
[55] Conder, J. M.; Hoke, R. A.; Wolf, W. d.; Russell, M. H.; Buck, R. C. Are PFCAs bioaccumulative? A critical review and comparison with regulatory criteria and persistent lipophilic compounds. *Environmental science & technology* **2008,** *42* (4), 995-1003.
[56] Houde, M.; Martin, J. W.; Letcher, R. J.; Solomon, K. R.; Muir, D. C. Biological monitoring of polyfluoroalkyl substances: a review. *Environmental science & technology* **2006,** *40* (11), 3463-3473.
[57] Kudo, N.; Kawashima, Y. Toxicity and toxicokinetics of perfluorooctanoic acid in humans and animals. *The Journal of toxicological sciences* **2003,** *28* (2), 49-57.
[58] Giesy, J. P.; Kannan, K. Global distribution of perfluorooctane sulfonate in wildlife. *Environmental science & technology* **2001,** *35* (7), 1339-1342.

[59] Darmanin, T.; Taffin de Givenchy, E.; Amigoni, S.; Guittard, F. Hydrocarbon versus fluorocarbon in the electrodeposition of superhydrophobic polymer films. *Langmuir* **2010,** *26* (22), 17596-17602.
[60] Rotenberg, B.; Patel, A. J.; Chandler, D. Molecular explanation for why talc surfaces can be both hydrophilic and hydrophobic. *J Am Chem Soc* **2011,** *133* (50), 20521-20527.
[61] Marmur, A. Wetting on Hydrophobic Rough Surfaces: To Be Heterogeneous or Not To Be? *Langmuir* **2003,** *19* (20), 8343-8348.

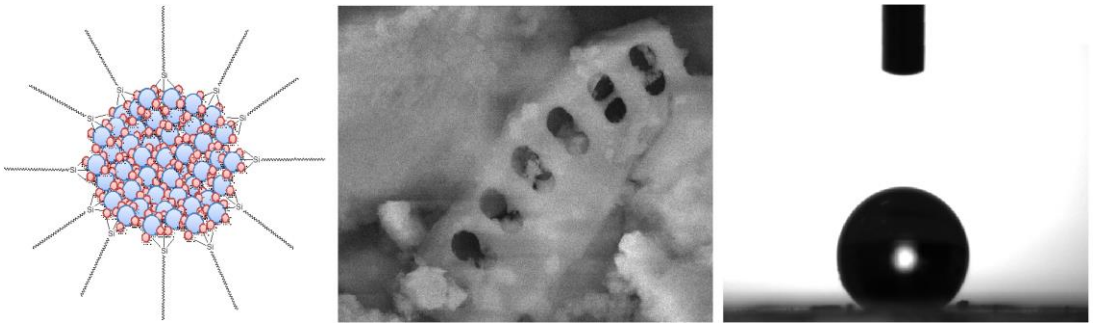

Table of Contents Graphic